Vibrating dichroic MEMS scanner based line scan multiphoton endomicroscope

Citation: Xu, Yingshun et al. "Vibrating dichroic MEMS scanner based line scan multiphoton endomicroscope." MOEMS and Miniaturized Systems XVIII, Proceedings of SPIE 10931, 1093116 (12 pages). © 2019 SPIE

As Published: http://dx.doi.org/10.1117/12.2510040

Publisher: Society of Photo-Optical Instrumentation Engineers (SPIE)

Persistent URL: https://hdl.handle.net/1721.1/129460

Version: Final published version: final published article, as it appeared in a journal, conference proceedings, or other formally published context

Vibrating dichroic MEMS scanner based line scan multiphoton endomicroscope

Xu, Yingshun, Cheng, Jin, Xu, Naitao, Zhu, Lanping, Cao, Yuzhu, et al.

Yingshun Xu, Jin Cheng, Naitao Xu, Lanping Zhu, Yuzhu Cao, Bei Fang, Xin Chen, Suogang Wang, Peter T. C. So, "Vibrating dichroic MEMS scanner based line scan multiphoton endomicroscope," Proc. SPIE 10931, MOEMS and Miniaturized Systems XVIII, 1093116 (4 March 2019); doi: 10.1117/12.2510040

SPIE.

Event: SPIE OPTO, 2019, San Francisco, California, United States

Vibrating dichroic MEMS scanner-based line scan multiphoton endomicroscope

Yingshun Xu*[a,b,c], Jin Cheng[d,e], Naitao Xu[e], Lanping Zhu[f], Yuzhu Cao[c], Bei Fang[c], Xin Chen[f], Suogang Wang[c] and Peter T. C. So*[a,b]

[a]Department of Mechanical Engineering, Massachusetts Institute of Technology, Cambridge, MA 02139, USA

[b]Department of Bioloical Engineering, Massachusetts Institute of Technology, Cambridge, MA 02139, USA

[c]School of Biomedical Engineering and Technology, Tianjin Medical University, Tianjin, 300071, China

[d]School of Optoelectronic Engineering, Xi'an Technological University, Xi'an, 710021, China

[e]MEMS Research and Development Center, China Key System Integrated Circuit Co., Ltd. (CKS), Wuxi, 214100, China

[f]Department of Gastroenterology and Hepatology, Tianjin Medical University General Hospital, Tianjin 300052, China

ABSTRACT

To achieve optical biopsy for gastro-intestinal (GI) endosopy with the use of nonlinear optical (NLO) endomicroscopes, integration of NLO technology with the design of a conventional flexible GI endoscope is necessary. One key challenge has been to design an NLO distal tip which can be compatible with flexible GI endoscopy retroflexion curvature radius as small as 20 mm to provide bending angle up to 210 degrees; the state-of-the-art NLO miniaturized design still consists of a long rigid "needle" shape probe at the distal end that can be damaged during the retroflex procedure when passing through the instrument channel of a flexible GI endoscope for *in vivo* imaging. To circumvent this design challenge, authors present a line scan multiphoton endomicroscope utilizing a novel simplified microelectromechanical systems (MEMS) scanner. This unique MEMS scanner consists of a customized single-axis dichroic MEMS scanner (SADMS) and vibrates at the back focal point of a customized micro-objective lens. This work demonstrates the new NLO scanner design can be compatible with conventional flexible GI endoscope to offer *in situ* functional microscopic imaging capability.

Keywords: micromirror, line scan, endomicroscope, multiphoton microscope, gastroenterology

1. INTRODUCTION

The concept of optical biopsy has been proposed in many decades, leading to development of novel endoscopic optical imaging technologies that can provide *in vivo* and *in situ* high resolution images offering either morphologic or functional or even both morphologic and functional features. Among them, NLO imaging, especially two-photon excited fluorescence (TPEF) [1-4], second harmonic generation (SHG) [5-7] as well as coherent stokes Raman scattering (CARS) [8-12] permit functional screening for endogenous contrasts including reduced nicotinamide adenine dinucleotide (NADH), collagens and lipids, promising potential of label-free imaging. Consequently, much research efforts have also been channeled to developing NLO endomicroscope. To date, most of the reported NLO endomicroscopes [13-23] are based on a fiber-scanning mechanism, which consists of a group of piezoelectric microactuators used to vibrate a photonic crystal excitation fiber for two-dimensional pattern generation. In detail, the length of the fiber-based piezoelectric microactuator assembly could be up to tens of millimeters for a sufficient scanning range. This assembly is

*Prof. Xu: xuy@mit.edu, xuyingshun@tmu.edu.cn; Prof. So: ptso@mit.edu

MOEMS and Miniaturized Systems XVIII, edited by Wibool Piyawattanametha, Yong-Hwa Park, Hans Zappe,
Proc. of SPIE Vol. 10931, 1093116 · © 2019 SPIE · CCC code: 0277-786X/19/$18 · doi: 10.1117/12.2510040

usually coupled with gradient refractive index (GRIN) lenses in tiny diameter or larger refractive optical lenses for used as micro-objective lenses. Due to these two design features, most of NLO endomicroscopes present their "needle" shapes and outline parameters of some designs are summarized in Table 1.

Table 1. Summary of some reported fiber scanning optical endomicroscopes for nonlinear imaging.

Publication	OD (mm)	Length of rigid part (mm)	Year
C. J. Engelbrecht et al [13]	1	~14	2008
R. Le Harzic et al [14]	~3	~22	2008
Y. Wu et al [15]	2.4	100	2009
Y. Zhao et al [16]	2.8	25	2010
D. R. Rivera et al [17]	3	40	2011
D. M. Huland et al [18]	1	80	2012
D. G. Ouzounov et al [19]	5	50	2013
G. Ducourthial et al [20]	2.2	37	2015
Y. Wang et al [21]	2	50	2016
F. Akhoundi et al [22]	5	40	2018
P. Zirak et al [23]	2.2	187	2018

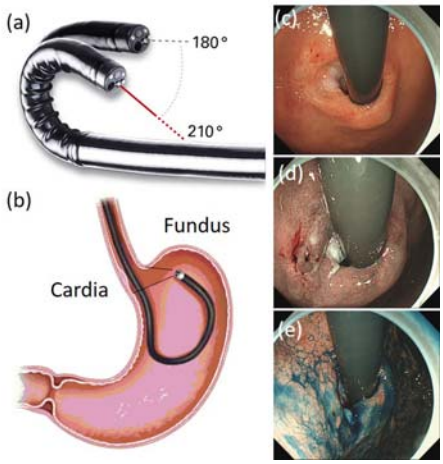

Figure 1. (a) Retroflexion of a flexible GI endoscope [24]; (b) Illustration of cardia inspection [25]; (c) White light endoscopic image, (d) Narrow Band Imaging (NBI) image and (e) Chromoendoscopic image of human cardia provided by Tianjin Medical University General Hospital (TMUGH).

In a typical gastroenterological imaging application, a physician operates a flexible GI endoscope and performs retroflexion to visibly investigate the surface of a patient's GI tract. An example of stomach cardia inspection by retroflexion of a flexible GI endoscope is shown in Figure 1. A flexible GI endoscope has mechanical joints of multi-degree-of-freedom (DOF) at the distal end and has one or two instrument channels for biopsy incision or other necessary operations. Table 2 summarizes specifications of a gastroscope and a colonoscope both of which are produced by Olympus [26, 27] as examples. Since parameters of bending sections shown in Table 2 are usually not officially revealed by endoscope vendors, these parameters are collected from compatible parts by third party vendors [28].

Table 2. Specifications of a gastroscope and a colonoscope.

Model	Endoscope Body			Bending Section [26]				
	Distal End Outer Diameter (mm)	Up/Down/ Right/Left (degrees)	Instrument Channel Internal Diameter (mm)	Outer Diameter (mm)	Thickness (mm)	Inner Bore (mm)	Length (mm)	Material
Gastroscope GIF-Q180 [26]	8.8	210/90/ 100/100	2.8	8.5	0.4	5	68	S304 Stainless Steel
Colonoscope CF-H190L/I [27]	13.2	180/180/ 180/180	3.7	11.6	0.4	7.3	109	S304 Stainless Steel

Detailed information on mechanical structures of a bending section in a flexible GI endoscope will not be discussed in this article. Since the length of a bending section is fixed, shorter bending section length always results in smaller radius of curvature with the same bending angle. For example, Olympus GIF-Q180 with a shorter bending section length of 68 mm exhibits better flexibility than Olympus GIF-Q160 with a longer bending section length of 74 mm with the same bending angle. To access some imaging regions of a human GI tract, especially cardia and fundus of stomach, NLO endomicroscopes must be brought along with a flexible GI endoscope. However, even if the diameter of a NLO endomicroscope is less than the internal diameter of the instrument channel of a flexible GI endoscope, the long rigid part length of a fiber scanning NLO endomicroscope still may cause damages to itself or the flexible GI endoscope in the case of significant tip bending for typical cardia / fundus investigation and make it impossible for clinical applications. Experimental illustration of apparently limited bending capability of needle gauge inserted flexible GI endoscope has been demonstrated [29].

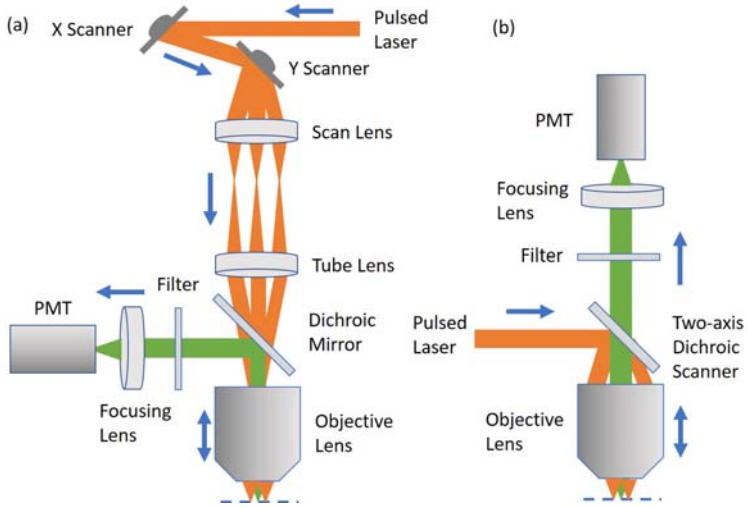

Figure 2. Illustration of structures of (a) a point scanning NLO microscope and (b) a dichroic scanner-based point scanning NLO microscope.

To solve the aforementioned issue and develop a NLO endomicroscope which is truly workable with a flexible GI endoscope without any loss of flexibility, authors aim to provide a scanning NLO endomicroscope with much shorter rigid part length in comparison with reported fiber scanning counterparts. The first attempt for this goal [30] is directly downsizing a benchtop NLO microscope whose structure is shown in Figure 2 (a). In this design a two-axis commercial MEMS scanner is used to function as the X-Y scanner pair in a benchtop NLO microscope. The resulted overall

dimension of the streamlined cubic shape NLO endomicroscope is about 15.5 mm by 12.9 mm by 10 mm. It almost fully blocks all functional ports and occupies all two instrument channels of an Olympus 2TQ260M gastroendoscope. Moreover, it is found to be difficult to reduce its size in further. As further developments, authors reported a novel idea of dichroic scanner based NLO microscope whose structure is shown in Figure 2 (b). In this concept reflective scanners are replaced by a conceptual two-axis dichroic scanner and hence both the scan lens and the tube lens are removed. This idea was preliminarily demonstrated by a modified commercial MEMS scanner mounted with an external tiny dichroic plate for dynamic loading tests [31].

In this article authors present a novel line scan NLO endomicroscope based on a highly customized single axis dichroic scanner, highlighting its short rigid part length of less than 7.5 mm. Due to the back focal plane scanning mechanism of this concept, commercially available micro-objective lenses are not compatible. Detailed information on the customized micro-objective lens and focusing lens is also provided in following sections of this article.

2. METHODOLOGY

2.1 Structure of a benchtop dichroic scanner-based line scan NLO microscope

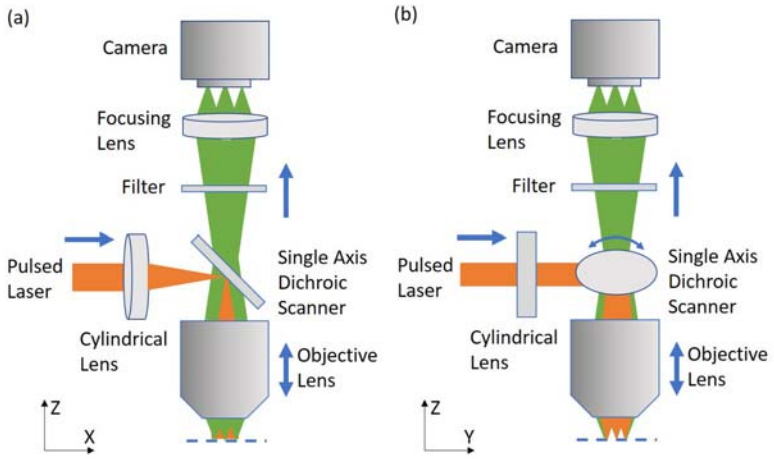

Figure 3. (a) X-Z and (b) Y-Z views of a dichroic scanner-based line scan NLO microscope.

As shown in Figure 3 (a) and (b), a dichroic scanner-based line scan NLO microscope consists of a cylindrical lens, a SADMS, a customized high numerical aperture (NA) infinite-corrected objective lens featuring external back focal plane, an emission filter, a focusing lens and a CMOS camera working with a rolling shutter. The cylindrical lens forms the incident pulsed laser into a line focus onto the SADMS. The SADMS is rotating at the back focal plane of the objective and generates a line focus in Y direction. The objective lens converts the line focus in Y direction onto line foci in X direction in the front focal plane. The rotation axis of the SADMS lies in the same plane with the X direction. Therefore, the SADMS moves the line focus along the Y direction to form a two-dimensional focal plane. NLO signals excited from each focus point in this two-dimensional focal plane is collected by the same objective lens, passing through the SADMS and then focused by a focusing lens. The focusing lens also generates line foci in X direction which are moving in Y direction. The rolling shutter of a CMOS camera is synchronized with the dichroic scanner as a virtual slit [32]. A high-speed line scan imaging utilizes the line by line readout of line foci of NLO signals in the X direction by the CMOS camera.

2.2 Structures of dichroic MEMS scanner-based line scan NLO endomicroscopes (DMS-LS-NLOE)

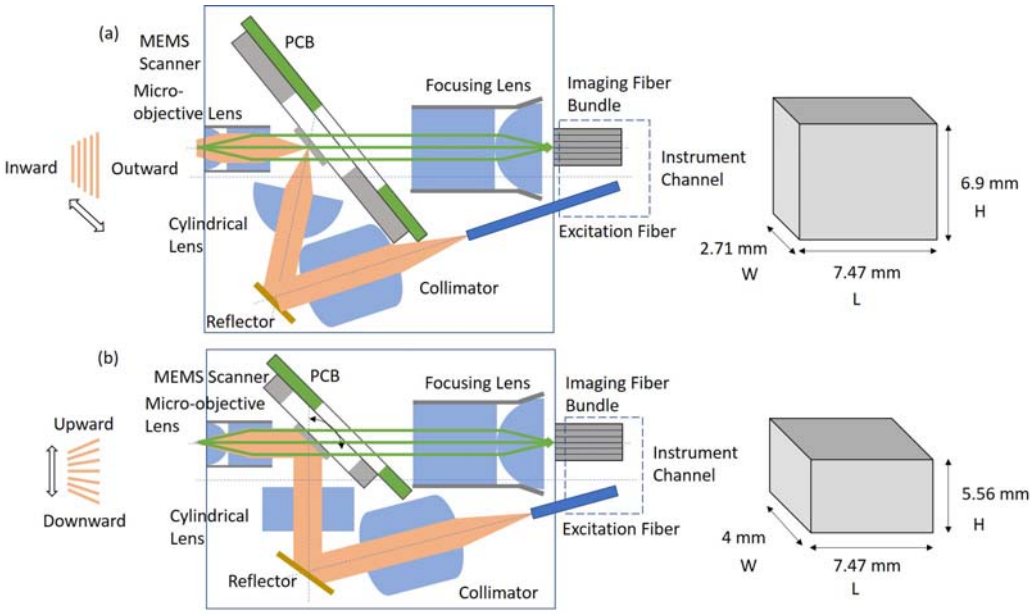

Figure 4. Illustration of two types of DMS-LS-NLOE of (a) Type A design with a vertically placed MEMS scanner and (b) Type B design with a transversely placed MEMS scanner.

In this article authors presents two possible types of DMS-LS-NLOE as shown in Figure 4 (a) and (b). It should be noted that width values (W) shown in Figure 4 does not include a waterproof shell surrounding assembled components. Main differences between them lie in directions of both the SADMS as well as the cylindrical lens. The rotation axis of the SADMS must be contained in the sagittal plane of the cylindrical lens. Like the benchtop system mentioned above, each of both two types of DMS-LS-NLOE also consists of a cylindrical lens, a SADMS with a PCB, a micro-objective lens，a focusing lens, a reflector, an excitation fiber and an imaging fiber bundle. Detailed information for every component will be discussed in following sections. In the Type A design angles of the SADMS, the optical axis of the cylindrical lens and the optical axis of the collimator to the optical axis of the micro-objective lens are 50 degrees, 80 degrees and 17 degrees, respectively. In the Type B design these angles are 45 degrees, 90 degrees and 17 degrees, respectively.

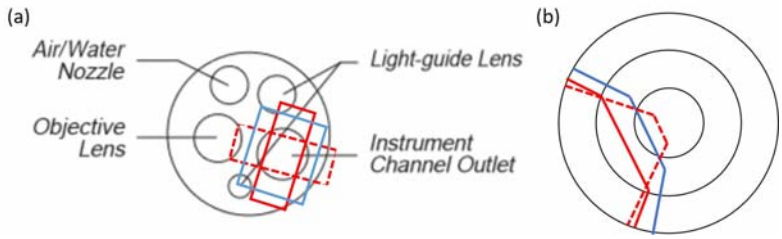

Figure 5. (a) Front view of an Olympus GIF-180 endoscope mounted with Type A design in tangential direction (solid red) and in radial direction (dashed red) as well as Type B design (solid blue); (b) Estimated shadows in the endoscope field of view.

Since outline dimensions of two types of DMS-LS-NLOE are shown in Figure 4, the Type A design has a flat rectangular prism shape while the Type B design is narrower but much thicker. An Olympus GIF-180 endoscope is used to demonstrate how a distally mounted DMS-LS-NLOE blocks the field of view (FOV) of the endoscope in Figure 5. The outer diameter of the Olympus GIF-180 endoscope is 9.8 mm and the inner diameter of its instrument channel is 2.8 mm. The FOV is 140 degrees while the depth of field (DoF) is 2 mm to 100 mm. The minimal visible distance of the object reaching out of the instrument channel is 3 mm from the distal end of the endoscope. In Figure 5 (a) three mounting configurations include a Type A design in tangential direction (solid red), a Type A design in radial direction (dashed red) and a Type B design (solid blue). According to the estimated shadow in the endoscope FOV caused by a mounted DMS-LS-NLOE shown in Figure 5 (b), the Type A design mounted in tangential direction blocks the smallest area in the FOV and occupies about 16 % of the FOV. It could be attributed to the largest distance between the mounted DMS-LS-NLOE and the objective lens in Type A design mounted in tangential direction. The DMS-LS-NLOE also

minimizes blockage of distal end functional ports of the endoscope due to its compact cross-sectional dimensions in comparison with authors' previous report [30]. As a conclusion, the Type A design is selected for further investigation in this article due to its flat shape for minimizing FOV blockage.

2.3 Single axis dichroic MEMS scanner

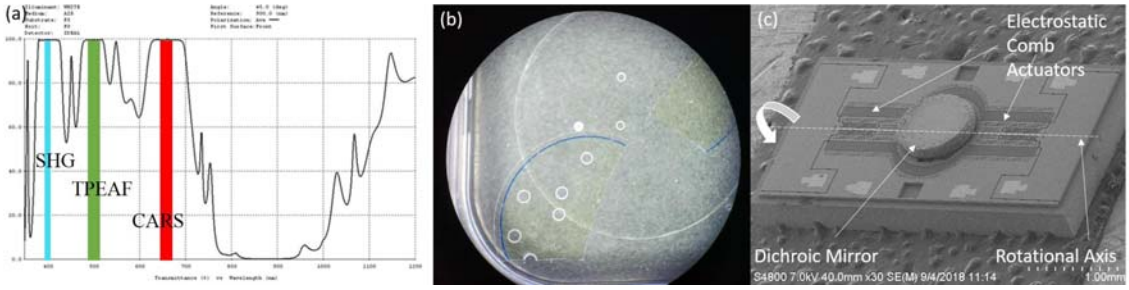

Figure 6. (a) Spectral curve of the dichroic coating; (b) Laser dicing of the dichroic mirror; (c) SEM micrograph of a SADMS.

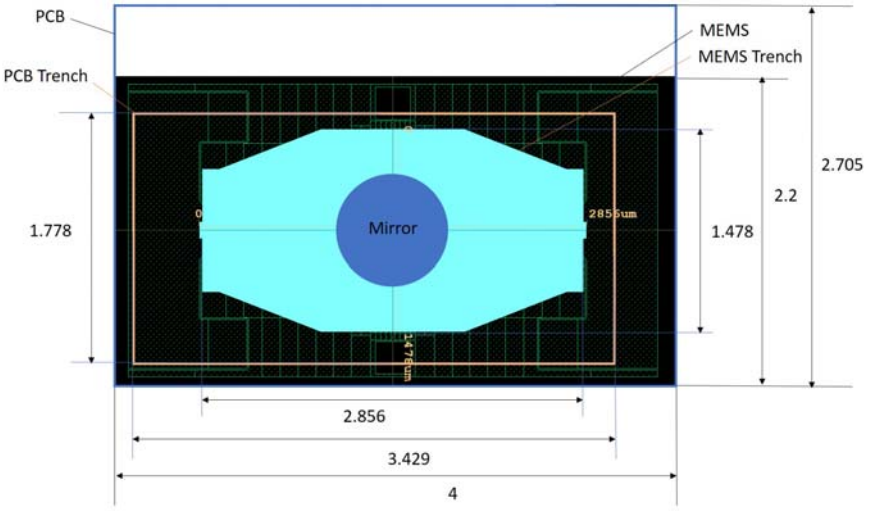

Figure 7. Dimensions of a SADMS, its backside DRIE trench, an attached PCB and PCB's trench. (Unit: mm)

An electrostatic comb drive-based SADMS is fabricated by a SOI fabrication process. The tiny quartz dichroic mirror made by laser dicing has a diameter of 0.8 mm and the thickness of 0.145 mm. The transmission curve of the dichroic plate customized for multimodal NLO detection is presented in Figure 6 (a). Laser dicing of a dichroic mirror and a SEM micrograph of a SADMS are shown in Figure 6 (b) and (c). Total outline dimensions of the SADMS is 4 mm by 2.2 mm by 0.5 mm shown in Figure 7 and its backside deep reactive-ion etching (DRIE) trench has dimensions of 2.856 mm by 1.478 mm. Distances between edges of the trench and the central dichroic mirror are critical and should be large enough to avoid blocking collected NLO light signals in large angles. Based on the optical simulation results presented in the section 2.5, the longer edge of 2.856 mm of the backside DRIE just allows the passage of collected NLO light signals in 20 degrees, which exactly fits the excitation angle of the micro-objective lens in the Type A. As a comparison, in the Type B design the shorter edge of 1.478 mm of the backside DRIE only allows the passage of collected NLO light signals in about 10 degrees, leading to significantly lower NLO signal collection efficiency as well as reduction of image size.

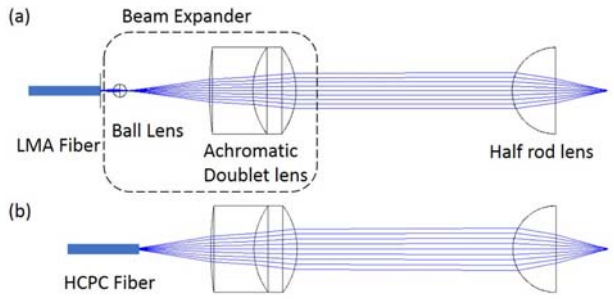

Figure 8. Schematics of the line focus forming optics for (a) a LMA fiber and (b) a HCPC fiber.

Two types of line focusing optics are developed for both hollow core photonic crystal (HCPC) fibers for single wavelength pulsed laser transmission and single mode large mode area (LMA) fibers for multi-wavelength laser transmission (usually required in CARS). In the first type, since the NA of the LMA fiber (LMA20, NKT Photonics) is ~0.04 at 800 nm excitation wavelength, the line focusing optics is built by a spherical lens (diameter=0.3 mm), an achromatic doublet lens (diameter=2 mm, f=3 mm) and a half rod lens (diameter=2 mm) which is cut into half from a rod lens, shown in Figure 7 (a). The ball lens and the achromatic doublet lens work as a beam expander in Keplerian telescope optics. The final resulted NA is about 0.17 and the working distance (WD) is ~1.2 mm. The formed line focus is projected on the dichroic plate of the SADMS. A reflective mirror plate between the beam expander and the half rod lens is not shown in Figure 8. In the second type shown in Figure 8 (b), it is much easier to deal with the diverging beam of a HCPC fiber (HC-800, NKT Photonics) with high NA of ~0.2 also at 800 nm excitation wavelength. Therefore, no beam expander required in this case.

2.4 Micro-objective lens and reimaging lens

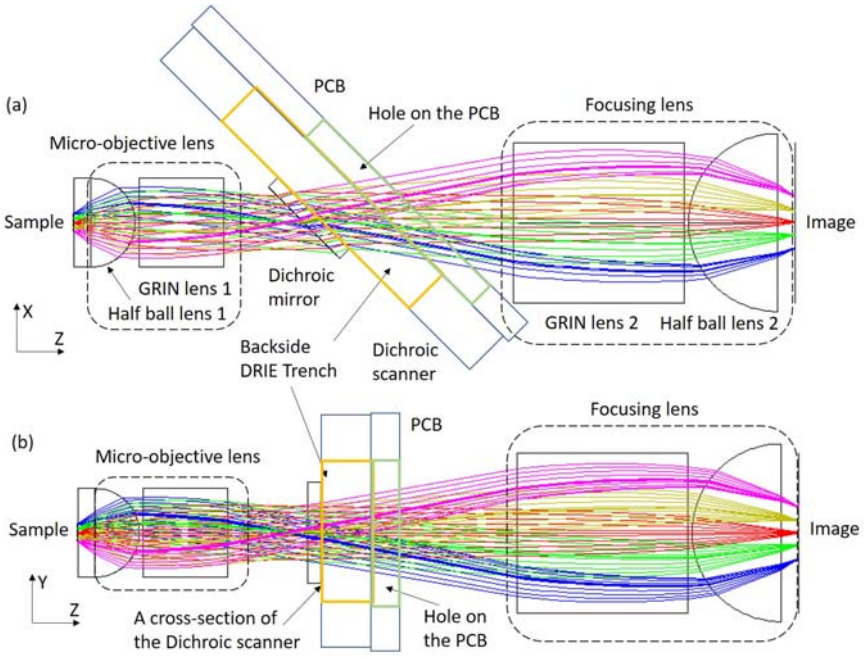

Figure 8. Schematics of the micro-objective lens and focusing lens in (a) X-Z view and (b) Y-Z view.

Different from other kinds of micro-objective lenses designed for conventional endoscopes [33-39], the micro-objective lens described in this article has been infinite-corrected, mid-high NA (~0.66), large angle of view (totally 20 degrees) and its back focal plane out of the lens body. Usually the back focal plane of a microscopic objective lens in middle to high NA always locates within the lens body due to its short focal length. It is not possible to directly steer laser beam at the back focal plane of the microscopic objective lens. That is why a pair of scan lens and tube lens are used to deliver scanning beam into the internal back focal plane of a microscopic objective lens. In this case the micro-objective lens

described in this article could be considered as a high NA scan lens. Due to size limitation for endoscopic applications, the structure of the micro-objective lens must be simple, and the number of lenses should be limited to 2-3 pieces. Tradeoff among lens size, imaging performance including NA and FOV and fabrication feasibility has been thoroughly investigated. As a result, in this case, the combination of a GRIN lens and a half ball lens is selected to balance all parameters as presented in Figure 9 (a) and (b). The X-Z view shown in Figure 8 (a) indicates the longer edge of the backside DRIE trench of a SADMS should be large enough, which has been concluded in the section 2.3. The hole in the PCB should be also biased in conjunction with the backside DRIE trench along the optical axis of the micro-objective lens. All optical components are commercially available while GRIN lenses have been cut into appropriate lengths to reach the best performance. As for the design of a focusing lens, N. A. Switz et al [33] discussed that a reversed mobile phone photographic lens could be used as a micro-objective lens and offer the possibility of extending a low cost, portable diagnostic microscope. Therefore, authors utilize the same combination of a GRIN lens and a half ball lens with different parameters due to the asymmetrical structure discussed below. Parameters of both the micro-objective lens and focusing lens have been listed in Table. 3. Tiny stainless-steel tubes are used to precisely assemble all optical components together.

Table 3. Parameters of the micro-objective lens and the focusing lens.

Items		Micro-objective lens	Focusing lens
Half ball lens	Diameters (mm)	1	2
	Material	Sapphire	N-BK7
GRIN lens	Diameter (mm)	1	1.8
	Length (mm)	0.95	1.92
Total Length (mm)		1.45	2.92

A dichroic mirror is inserted between two micro compound lenses and its exact position coincides with external back focal planes of both the micro-objective lens and the focusing lens. Considering the biased position of the mounted dichroic mirror as well as the thickness of both the MEMS scanner (~500 um thickness) and the ultrathin PCB (~350 um thickness) attached below, it forms an asymmetrical structure of the DMS-LS-NLOE and leads to a focusing lens having a larger size. However, a near symmetrical structure with similar sizes of both the objective lens and the focusing lens may appear in a benchtop counterpart shown in Figure 3.

2.5 Assembly and packaging

All components are precisely aligned and assembled by two pieces of micromachined silicon optical bench (SiOB). Both DRIE etching and anisotropic wet etching are used to form trenches in SiOBs. Similar research has been done for endoscopic optical coherence tomography (EOCT) application [40] taking its advantages of high precision and mass productivity. SiOB technology performs far better fabrication precision than popular 3D polymer printing techniques.

3. PRELIMINARY CHARACTERIZATION

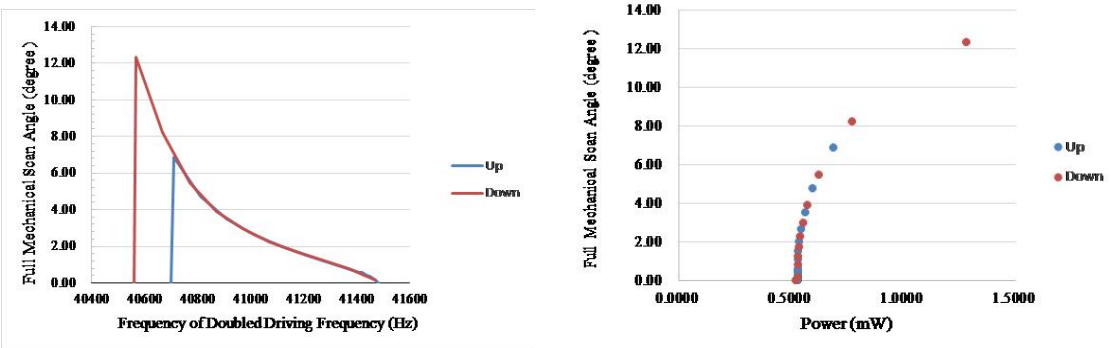

Figure 10. (a) the frequency response and (b) the dynamic power consumption of a dichroic MEMS scanner.

Preliminary characterization results of a SADMS, including the frequency response and the dynamic power consumption, are shown in Figure 10 (a) and (b). The resonant frequency of the MEMS scanner is more than 20 KHz.

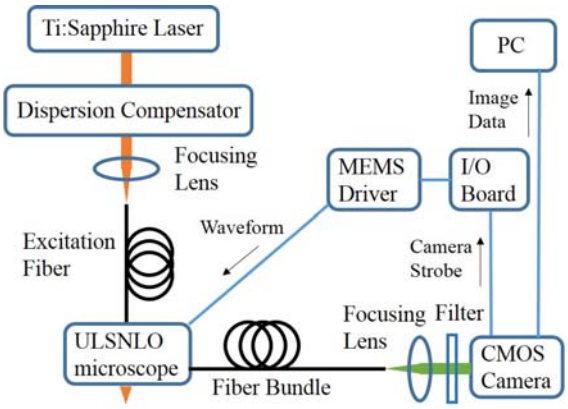

Figure 11. Schematics of the whole DMS-LS-NLOE imaging system.

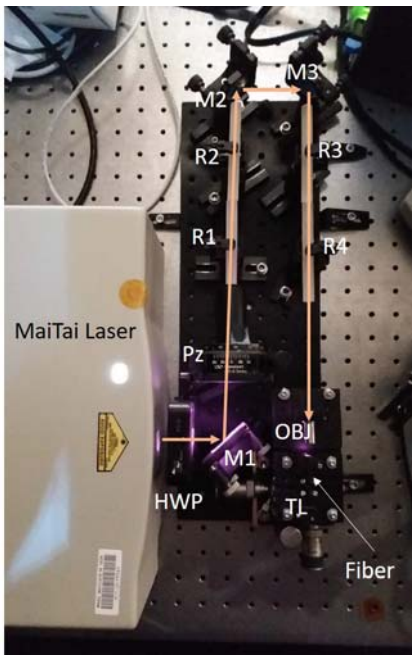

Figure 12. Compact optical setup for power adjustment, dispersion compensation and fiber coupling. HWP: Half wave plate; M1-M3: Mirror; Pz: Polarizer; R1-R4: Glass rod; OBJ: Objective; TL: Translational stage.

Figure 11 shows the schematics of the whole DMS-LS-NLOE imaging system while Figure 12 shows a detailed photo on a compact optical setup for power adjustment, dispersion compensation and fiber coupling based on a Spectral Physics MaiTai laser. The laser generates laser pulses with the width of about 75 fs and the repetition rate of 80 MHz. Before coupled into a 1 meter length HCPC fiber (HC-800, NKT Photonics) by an objective lens (C610TME-B，NA=0.6, Thorlabs) mounted on a 3-axis fiber launch system (MBT612D/M, Thorlabs) , the output laser tuned at 800 nm pass through a half wave plate (10RP02-46, Newport) and a polarizer (10GL08AR, Newport) for power adjustment and then a series of customized glass tubes (N-SF66, Schott) to compensate the anomalous group velocity dispersion (GVD) caused mainly by the long PCF.

CONCLUSION

In this article authors presents a novel DMS-LS-NLOE based on a highly customized SADMS, highlighting its short rigid part length of less than 7.5 mm. Customized micro-objective lens and focusing lens for back focal plane scanning are also developed featuring their ultrasmall dimensions.

ACKNOWLEDGEMENTS

This research was supported in part by the Science and Technology Development Fund of Tianjin Education Commission for Higher Education under Grant 2017JK232 and in part by the Chinese Scholarship Council under Grant 201706945010.

REFERENCES

[1] Lu, R. W., Li, Y. C., Ye, T., Strang, C. E., Keyser, K. T., Curcio, C. A., and Yao, X., "Two-photon excited autofluorescence imaging of freshly isolated frog retinas," Biomedical Optics Express, 2(6), 1494-1503. Biomed Opt Express, 2(6): 1494–1503 (2011).

[2] Han, M., Bindewaldwittich, A., Holz, F. G., Giese, G., Niemz, M. H., Snyder, S. R., Sun, H., Yu, J., Agopov, M., Schiazza, O.L., Bille, J. F., "Two−photon excited autofluorescence imaging of human retinal pigment epithelial cells," Journal of Biomedical Optics, 11(1), 010501 (2006).

[3] Sharma, R., Williams, D. R., Palczewska, G., Palczewski, K., and Hunter, J. J, "Two-Photon Autofluorescence Imaging Reveals Cellular Structures Throughout the Retina of the Living Primate Eye," Investigative Ophthalmology & Visual Science, 57(2), 632-646 (2016).

[4] Zheng, W., Wu, Y., Li, D., and Qu, J. Y., "Autofluorescence of epithelial tissue: single-photon versus two-photon excitation," Journal of Biomedical Optics, 13(5), 054010 (2008).

[5] Chen, X., Nadiarynkh, O., Plotnikov, S. V., and Campagnola, P. J., "Second harmonic generation microscopy for quantitative analysis of collagen fibrillar structure," Nature Protocols, 7(4), 654-669 (2012).

[6] Williams, R. M., Zipfel, W. R., and Webb, W. W., "Interpreting Second-Harmonic Generation Images of Collagen I Fibrils," Biophysical Journal, 88(2), 1377-1386 (2005).

[7] Han, M., Giese, G., and Bille, J. F., "Second harmonic generation imaging of collagen fibrils in cornea and sclera," Optics Express, 13(15), 5791-5797 (2005).

[8] Cheng, J., Volkmer, A., Book, L. D., and Xie, X. S., "An Epi-Detected Coherent Anti-Stokes Raman Scattering (E-CARS) Microscope with High Spectral Resolution and High Sensitivity," Journal of Physical Chemistry B, 105(7), 1277-1280 (2001).

[9] Evans, C. L., Potma, E. O., Puorishaag, M., Cote, D., Lin, C. P., and Xie, X. S., "Chemical imaging of tissue in vivo with video-rate coherent anti-Stokes Raman scattering microscopy," Proceedings of the National Academy of Sciences of the United States of America, 102(46), 16807-16812 (2005).

[10] Wang, H. W., Langohr, I. M., Sturek, M., and Cheng, J., "Imaging and Quantitative Analysis of Atherosclerotic Lesions by CARS-Based Multimodal Nonlinear Optical Microscopy," Arteriosclerosis, Thrombosis, and Vascular Biology, 29(9), 1342-1348 (2009).

[11] Le, T. T., Rehrer, C. W., Huff, T. B., Nichols, M. B., Camarillo, I. G., and Cheng, J., "Nonlinear optical imaging to evaluate the impact of obesity on mammary gland and tumor stroma," Molecular Imaging, 6(3), 205-211 (2007).

[12] Cheng, J., Jia, Y. K., Zheng, G., and Xie, X. S., "Laser-scanning coherent anti-Stokes Raman scattering microscopy and applications to cell biology," Biophysical Journal, 83(1), 502-509 (2002).

[13] Engelbrecht, C. J., Johnston, R. S., Seibel, E. J., and Helmchen, F., "Ultra-compact fiber-optic two-photon microscope for functional fluorescence imaging in vivo, " Optics Express, 16(8), 5556-5564 (2008).

[14] Harzic, R. L., Weinigel, M., Riemann, I., Konig, K., and Messerschmidt, B., "Nonlinear optical endoscope based on a compact two axes piezo scanner and a miniature objective lens, " Optics Express, 16(25), 20588-20596 (2008).

[15] Wu, Y., Leng, Y., Xi, J., and Li, X., "Scanning all-fiber-optic endomicroscopy system for 3D nonlinear optical imaging of biological tissues, " Optics Express, 17(10), 7907-7915 (2009).

[16] Zhao, Y., Nakamura, H., and Gordon, R. J., "Development of a versatile two-photon endoscope for biological imaging, " Biomedical Optics Express, 1(4), 1159-1172 (2010).

[17] Rivera, D. R., Brown, C. M., Ouzounov, D. G., Pavlova, I., Kobat, D., Webb, W. W., and Xu, C., "Compact and flexible raster scanning multiphoton endoscope capable of imaging unstained tissue, " Proceedings of the National Academy of Sciences of the United States of America, 108(43), 17598-17603 (2011).
[18] Huland, D. M., Brown, C. M., Howard, S. S., Ouzounov, D. G., Pavlova, I., Wang, K., Rivera, D.R., Webb, W. W., and Xu, C., "In vivo imaging of unstained tissues using long gradient index lens multiphoton endoscopic systems, " Biomedical Optics Express, 3(5), 1077-1085 (2012).
[19] Ouzounov, D. G., Rivera, D. R., Williams, W. O., Stupinski, J. A., Southard, T. L., Hume, K. H., Bentley, J., Weiss, R. S., Webb, W. W. and Xu, C., "Dual modality endomicroscope with optical zoom capability, " Biomedical Optics Express, 4(9), 1494-1503 (2013).
[20] Ducourthial, G., Leclerc, P., Mansuryan, T., Fabert, M., Brevier, J., Habert, R., Braud, F., Batrin, R., Veverbizet, C., Bourgheckly, G., Thiberville, L., Druilhe, A., Kudlinski, A., and Louradour, F., "Development of a real-time flexible multiphoton microendoscope for label-free imaging in a live animal, " Scientific Reports, 5(1), 18303-18303 (2016).
[21] Akhoundi, F., Qin, Y., Peyghambarian, N., Barton, J. K., and Kieu, K., "Compact fiber-based multi-photon endoscope working at 1700 nm, " Biomedical Optics Express, 9(5), 2326-2335 (2018).
[22] Wang, Y., Li, Z., Liang, X., and Fu, L., "Four-plate piezoelectric actuator driving a large-diameter special optical fiber for nonlinear optical microendoscopy, " Optics Express, 24(17), 19949-19960 (2016).
[23] Zirak,P., Matz, G., Messerschmidt,B., Meyer, T., Schmitt, M., Popp,J., Uckermann, O., Galli, R., Kirsch, M., Winterhalder, M J., Zumbusch, A., "A rigid coherent anti-Stokes Raman scattering endoscope with high resolution and a large field of view, " APL Photonics. 3, 092409 (2018).
[24] PENTAX Endoscope Webpage https://www.pentaxmedical.com/pentax/en/101/1/RetroView-EC-3490Ti-Video-Colonoscope.
[25] Gaur P. and Dickinson K.J. "Esophageal Anatomy as Seen During Endoscopy and Basic Endoscopic Orientation. In: Blackmon S.H., Kim M.P., Dickinson K.J. (eds) Atlas of Esophageal Disease and Intervention," Springer, New York, NY (2015).
[26] Olympus GIF-Q180 Brochure https://medical.olympusamerica.com/sites/us/files/pdf/GIF-Q180_Brochure.pdf.
[27] Olympus Endoscope Overview 2018-2019 https://www.olympus.co.uk/medical/rmt/media/en-gb/Content/Content-MSD/Documents/Brochures/ENDOSCOPE-OVERVIEW-2017-2018.pdf.
[28] Olympus endoscope bending section vendor information https://www.alibaba.com/product-detail/GIF-Q150-Four-Directional-bending-section_60738538952.html?spm=a2700.7724838.2017005.2.3a2bb31b5AVXzR.
[29] O'Shea C., Ali K. K., Tugwell J., Kennedy M. P. and Cantillon-Murphy P. J. "The Effects of Occupying the Working Channel on Endoscopic Manipulation, " Annual meeting of the society of American gastrointestinal and endoscopic surgeons (2016).
[30] Xu Y., Xu N., Yang Y., Cheng J., Zhu L., Zeng F., Wang S., Cao Y., Chen X., Wang S. and Liu S., "Miniaturized scanning optical probe for multimodal nonlinear endomicroscopic imaging, " IEEE International Conference on Optical MEMS and Nanophotonics (OMN), pp.133-134 (2018).
[31] Xu Y., Cheng J. and Xu N., "Vibrating dichroic MEMS scanner towards ultrasmall laser scanning microscopes, " IEEE International Conference on Optical MEMS and Nanophotonics (OMN), pp.131-132 (2018).
[32] Hughes M. and Yang G., "Line-scanning fiber bundle endoscopy with a virtual detector slit, " Biomedical Optics Express 7(6), 2257-2268 (2016).
[33] Switz, N. A., D'Ambrosio, M. V., and Fletcher, D. A., "Low-cost mobile phone microscopy with a reversed mobile phone camera lens, " PLoS ONE 9(5), e95330 (2014).
[34] Jabbour, J. M., Bentley, J., Malik, B. H., Nemechek, J., Warda, J., Cuenca, R., Cheng, S., Jo, J. A., Maitland, K. C. "Reflectance confocal endomicroscope with optical axial scanning for in vivo imaging of the oral mucosa," Biomedical Optics Express, 5(11), 3781-3791 (2014).
[35] Wang, J., Li, H., Tian, G., Deng, Y., Liu, Q. and Fu, L., "Near-infrared probe-based confocal microendoscope for deep-tissue imaging," Biomedical Optics Express, 9(10), 5011-5025 (2018).
[36] Yang, L., Wang, J., Tian, G., Yuan, J., Liu, Q., and Fu, L., "Five-lens, easy-to-implement miniature objective for a fluorescence confocal microendoscope,", Optics Express, 24(1), 473-484 (2016).
[37] Matz, G., Messerschmidt, B., Gobel, W., Filser, S., Betz, C. S., Kirsch, M., Uckermann, O., Kunze, M., Flamig, S., Ehrhardt, A., Irion, K., Haack, M., Dorostkar, M. M., Herms, J., Gross, H., "Chip-on-the-tip compact

flexible endoscopic epifluorescence video-microscope for in-vivo imaging in medicine and biomedical research," Biomedical Optics Express, 8(7), 3329-3342 (2017).
[38] Wong, C., Pawlowski, M. E., Forcucci, A., Majors, C. E., Richardskortum, R., and Tkaczyk, T. S., "Development of a universal, tunable, miniature fluorescence microscope for use at the point of care," Biomedical Optics Express, 9(3), 1041-1056 (2018).
[39] Li, A., Hall, G., Chen D., Liang, W., Ning B., Guan H., and Li X., "A biopsy‐needle compatible varifocal multiphoton rigid probe for depth‐resolved optical biopsy," Journal of Biophotonics, e201800229 (2018).
[40] Xu Y., Wang M-F., Premachandran C. S., Chen K. W. S., Chen N. and Olivo M., "Platinum microheater integrated silicon optical bench assembly for endoscopic optical coherence tomography" Journal of Micromechanics and Microengineering, 20(1), 015008 (2010).